Journal of Quantitative Spectroscopy & Radiative Transfer 206 (2018) 36–45

Contents lists available at ScienceDirect

Journal of Quantitative Spectroscopy & Radiative Transfer

journal homepage: www.elsevier.com/locate/jqsrt

High temperature infrared absorption cross sections of methane near 3.4 μm in Ar and CO_2 mixtures

Batikan Koroglu[a,b], Sneha Neupane[a], Owen Pryor[a], Robert E. Peale[c], Subith S. Vasu[a,*]

[a] Physical and Life Sciences, Lawrence Livermore National Laboratory, Livermore, CA, 94550, USA
[b] Mechanical and Aerospace Engineering, Center for Advanced Turbomachinery and Energy Research (CATER), University of Central Florida, Orlando, FL 32816, USA
[c] Department of Physics, University of Central Florida, Orlando FL, 32816 USA

ARTICLE INFO

Article history:
Received 3 June 2017
Revised 15 October 2017
Accepted 3 November 2017
Available online 4 November 2017

ABSTRACT

The absorption cross-sections of CH_4 at two wavelengths in the mid-IR region: $\lambda_{peak} = 3403.4$ nm and $\lambda_{valley} = 3403.7$ nm were measured. Data were taken using three different compositions of non-reactive gas mixtures comprising $CH_4/Ar/CO_2$ between $700 < T < 2000$ K and $0.1 < P < 1.5$ atm in a shock tube utilizing a continuous-wave distributed-feedback quantum cascade laser. Also, broadband room temperature methane cross section measurements were performed using a Fourier transform infrared spectrometer and the cascade laser to gain a better insight into the changes of the line shapes in various bath gasses (Ar, CO_2, and N_2). An application of the high-temperature cross-section data was demonstrated to determine the concentration of methane during oxy-methane combustion in a mixture of CO_2, O_2, and Ar. Current measurements will be valuable addition to the spectroscopy database for methane- an important fuel used for power generation and heating around the world.

1. Introduction

Combustion of natural gas creates copious CO_2 and NO_x emissions. One possible solution for preventing NO_x emissions is the oxy-methane combustion with large CO_2 dilution. By using pure oxygen instead of air, resulting products can be reduced to mainly CO_2 and H_2O. CO_2 can then be captured and returned to the combustor to dilute the mixture again, transported via pipeline, or stored underground. The major concern with this nascent technology is the difference in methane combustion in air vs CO_2 containing gas mixtures. Recently, several research groups [1–5] studied the effects of carbon dioxide gas on the oxy-methane combustion. The present authors [1] investigated ignition delay times and concentration time histories in a shock tube and revealed changes in methane absorption cross sections around 3403 nm when the amount of carbon dioxide in the gas mixture of $CH_4/Ar/CO_2$ was increased from 0 to 30%. Accurate knowledge of the cross sections is essential for measuring concentrations using absorption spectroscopy. Therefore, the current study investigates the high temperature ($700 < T < 2000$ K) absorption cross sections of methane in gas mixtures containing various percentages of CO_2 gas (0, 30, and 98%).

Recent studies report methane detection at mid-infrared wavelengths for high temperature combustion applications. Sur et al. [6] developed a methane detection scheme using two absorption lines (on-line minus off-line) in the R branch of ν_3 band around 3175.8 nm and applied the technique to quantify methane concentration during C_3H_8 pyrolysis in shock tube experiments. Further work by Sajid et al. [7] used a quantum cascade laser and performed a differential wavelength scheme (peak minus valley) in the Q branch of ν_4 band around 7671.7 nm. The P branch of ν_3 band (asymmetric stretch) has also narrow and strong absorption lines which were utilized by Pyun et al. for developing interference-free detection of methane during n-heptane pyrolysis in shock tube experiments [8–10]. This detection scheme ($\lambda_{peak} = 3403.4$ nm and $\lambda_{valley} = 3403.7$ nm) was utilized by the present authors for methane concentration measurements during the pyrolysis of propionaldehyde [11]. In this study, methane cross sections in various bath gasses (e.g. Ar, CO_2, N_2) were studied using the same wavelength pair.

The effects of CO_2 on line intensities, pressure broadening, and narrowing coefficients of methane have been investigated by recent studies at different wavelengths in the mid-IR. Es-sebbar and Farooq [12] measured the aforementioned parameters for nine transitions of the P(11) manifold in the ν_3 band of methane between 3438.8 and 3442.3 nm at 297 K using N_2, H_2, He, Ar, and CO_2 bath gases. Lyulin et al. [13] studied CO_2 line broadening and pres-

* Corresponding author.
E-mail address: subith@ucf.edu (S.S. Vasu).

https://doi.org/10.1016/j.jqsrt.2017.11.003
0022-4073/

Table 1
FTIR Spectrometer Configuration.

Light source	Globar
Beamsplitter	Potassium bromide (KBr)
Detector	MCT HgCdTe
Pressure gauge	Baratron (±0.05% accuracy)
Optical path length	10 cm
FTIR input aperture	3 mm
Resolution	0.1 cm^{-1}
Phase correction, Zero-filling	Mertz, 4 × zero-filling
Apodization function	Boxcar

sure induced shift coefficients of methane spectral lines between 1628.7 and 1801.8 nm region at room temperature. In addition, Fissiaux et al. [14] used a tunable diode-laser spectrometer and examined the CO_2 broadening coefficients of 28 lines in the ν_4 band of CH_4 between 7305.1 and 8052.8 nm. There are also studies comparing the effect of different perturbing species (e.g. Ar, He, and N_2) on the absorption cross sections of methane using a He-Ne laser at fixed 3392 nm wavelength [15]. There is no report, to the best of our knowledge, on the absorption cross sections of methane measured in CO_2 bath gas around 3403 nm.

In this study, we performed methane cross section measurements in three bath gasses (N_2, Ar, and CO_2) at room temperature (296 K) and atmospheric pressure between 3402 and 3405 nm using an FTIR. These measurements helped us understand the changes in the cross sections of methane in different perturbing species. We also measured the absorption cross sections of methane near the P(8) line in ν_3 band at two wavelengths ($\lambda_{peak} = 3403.4$ nm and $\lambda_{valley} = 3403.7$ nm) at high temperatures ($700 < T < 2000$ K). These measurements were performed using a shock tube at pressures between $0.1 < P < 1.5$ atm with gas mixtures containing CH_4, CO_2, and Ar. An application of the recorded data is shown at the end of this paper. Interference-free determination of methane concentration was accomplished during a combustion reaction in CO_2-diluted gas mixtures. Therefore, the measured cross section data at the chosen wavelength pair can be utilized to perform concentration measurements in gas mixtures of $CH_4/O_2/CO_2/Ar$.

2. Experimental setup and procedure

2.1. Room temperature FTIR measurements

Absorption cross sections of methane were measured in N_2, Ar, and CO_2 bath gasses at 296 K and 1 atm. The spectra were recorded over the wavelength range between 3402 and 3405 nm using a vacuum bench Bomem DA8 Fourier Transform Infrared spectrometer described previously elsewhere [16]. The configuration of the FTIR is given in Table 1. Each spectrum was calculated by Fourier transform of 600 co-added interferograms.

2.2. Shock tube facility

The details of the double-diaphragm, heated, shock tube facility at UCF can be found in recent publications [1,11]. The shock tube has inside diameter of 14.17 cm. A piezoelectric pressure transducer (Kistler 603B1) was used to measure the pressure in the incident and reflected shock regions. Five piezoelectric pressure transducers (PCB 113B26; 500 kHz frequency response) connected to four time-interval counters (Agilent 53220A; 0.1 ns time resolution) were placed along the last 1.4 m of the shock tube to monitor the normal shock wave passage and thus to measure the incident shock velocities, which were then linearly extrapolated to the end wall. The temperature (T_5) and pressure (P_5) in the reflected shock region were calculated based on the extrapolated end wall shock velocity by using one dimensional ideal shock relations [17] and assuming chemically frozen and vibrationally equilibrated gasses. The incident shock wave attenuation was always found to be less than 1%/m. The uncertainty in the reflected shock temperature and pressure were estimated to be less than ± 2%.

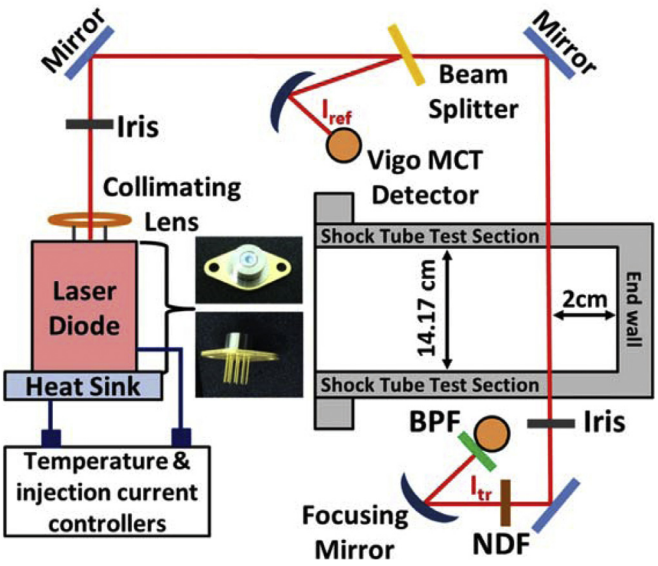

Fig. 1. The schematic of the end section of the shock tube with the laser and the optical components at a 2 cm sidewall location (BPF = Band Pass Filter, NDF = Neutral Density Filter).

2.3. Fuel/oxidizer mixture preparation

Before mixture preparation and shock tests, shock tube and the mixing facility were evacuated by a turbo molecular pump system (Agilent model V301) together with three rotary vane pumps (Agilent DS102). Before any experiment was conducted, pressure inside the shock tube setup was brought to $1x10^{-5}$ Torr. The test gases for current experiments were prepared in a 0.033 m^3 teflon-coated stainless steel high purity mixing facility. Different mixtures were created manometrically and then mixed overnight with a magnetically driven stirrer to ensure homogeneity. Pressures were measured using a 100 Torr (MKS Instruments/Baratron E27D, accuracy of 0.12% of reading) and 10,000 Torr (MKS Instruments/Baratron 628D, accuracy of 0.25% of reading) full scale range capacitance manometers. Research grade Ar (99.999%), He (99.999%), O_2 (99.999%), CO_2 (99.999%), and CH_4 (99.999%) were supplied by Air Liquide.

2.4. High temperature CH_4 cross section measurements at 3403.4 and 3403.7 nm

A continuous wave distributed feedback inter-band cascade laser (Nanoplus DFB ICL) was used for measuring methane (CH_4) absorption cross sections. The two wavelengths were chosen near the P(8) line in ν_3 band ($\lambda_{peak} = 3403.4$ nm and $\lambda_{valley} = 3403.7$ nm). This wavelength region was preferred in earlier studies [1,10,11,18–20] for methane detection because methane has structurally resolved absorption features around 3.4 µm, whereas most hydrocarbons have constant absorption coefficients. Fig. 1 shows the schematic of the end section of the shock tube with the laser and optical components. The laser diode was collimated using a lens (Thorlabs C036TMEE) and a laser beam profiler (Spiricon Pyrocam-III). The laser diode was mounted on a heat sink (Nanoplus TO66 mount) which was also connected to temperature (Thorlabs TLD001) and injection current (Thorlabs TTC001)

Table 2
Compositions of gas mixtures used for high temperature cross section measurements.

Mixture Type	X_{CH_4}	X_{CO_2}	X_{Ar}
Mixture I	0.02	0.00	0.98
Mixture II	0.02	0.30	0.68
Mixture III	0.02	0.98	0.00

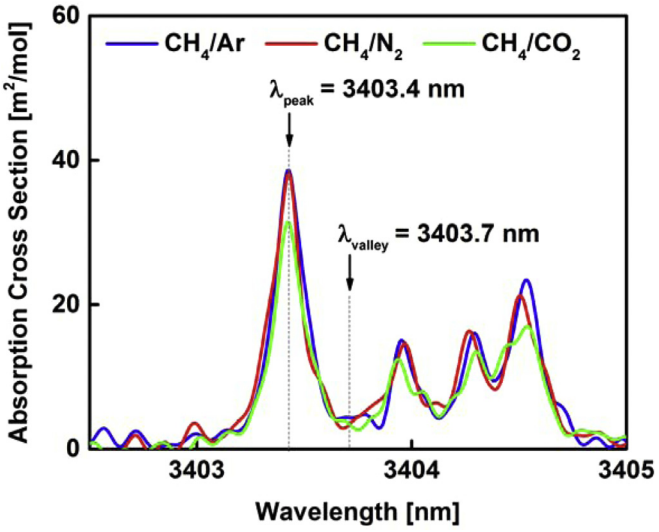

Fig. 2. Measured absorption spectra of CH_4 in different bath gasses (Ar, N_2, and CO_2) at 296 K and 1 atm.

controllers. A wavelength meter (Bristol 771 Spectrum Analyzer) was used to determine the variation of the output wavelength with temperature and current settings. The laser beam was split into two parts; a reference beam (I_{ref}) and the transmitted light (I_{tr}) that passes through the shock tube. Each beam was incident on a focusing mirror (Thorlabs CM254-050-P01), which helped minimize the beam-steering effects. Two thermoelectrically cooled HgCdTe (MCT) detectors (Vigo Systems PVI-2TE-3.4) were used. A fixed wavelength laser absorption measurement conducted in this study used the vacuum measurement to report the I_{ref} value. The transmitted beam was passed through an iris (Thorlabs ID25), neutral density filter (Thorlabs NDIR10A), and band pass filter (Thorlabs FB3500-500) to attenuate and minimize the interference on the detectors due to emission of gas species at high temperatures.

The ratio of transmitted and reference light intensities (I_{tr}/I_{ref}) were measured to obtain CH_4 absorption cross sections from Beer-Lambert law given by

$$\alpha_\nu = -\ln\left(\frac{I_{tr}}{I_{ref}}\right)_\nu = \sigma(\nu, T, P)\frac{P_{tot}}{RT}\chi L, \quad (1)$$

where α_ν is the absorbance, σ[cm^2/mol] is the absorption cross section of methane, P_{tot} [atm] is the total pressure within the system, and T [K] is the temperature of the gas, R [cm^{3}atm/K-mol] is the gas constant, L [cm] is the optical path length (shock tube inner diameter) and χ is the mole fraction of methane. Compositions of mixtures used for high temperature measurements are given in Table 2.

3. Results and discussion

3.1. Methane absorption cross sections at room temperature

Methane absorption spectra around 3 μm is shown in Fig. 2. Spectra were recorded using the FTIR at 296 K and 1 atm and using

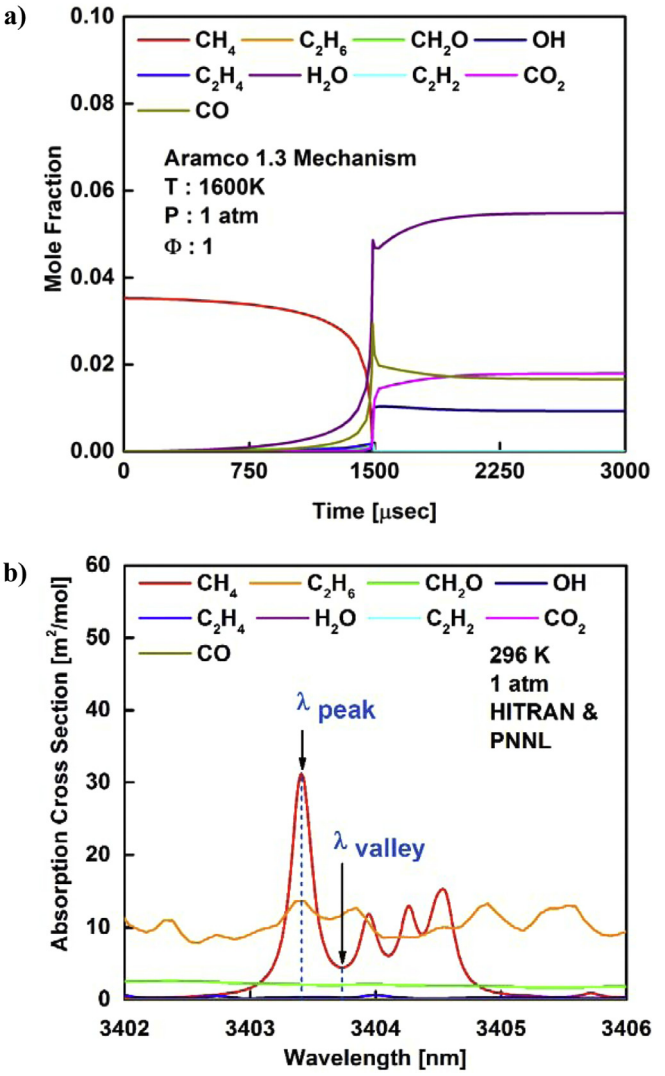

Fig. 3. (a) The Aramco 1.3 mechanism [13] prediction results for the main products of the ignition of 3.5% CH_4 and 7% O_2 in argon. (b) The absorption cross section values at 296 K and 1 atm are shown.

1% methane in three different bath gasses: Ar, N_2, and CO_2. Overall, methane cross sections are smaller in carbon dioxide bath gas. The line positions of the peak and valley wavelengths chosen for the shock tube measurements are noted in the figure. The cross sections measured in Ar and N_2 gasses at the peak wavelength were very similar (around 38.5 m^2/mol), whereas it decreased to 31.5 m^2/mol when measured in CO_2. However, we also repeated these measurements using our DFB-interband cascade laser to better resolve the changes in the line widths. Those results are discussed in Section 3.5.

Chemical kinetics simulations of methane combustion were performed to identify the main species that could interfere with methane detection around 3.4 μm. Due to its ability to closely predict the experimental results, Aramco 1.3 reaction mechanism [21] was used for this purpose. Shock tube experiments were modeled at constant volume and internal energy (constant-U,V) using the CHEMKIN PRO simulation tool [22]. Fig. 3(a) shows the prediction results as a function of time for the main products of ignition of stoichiometric methane and oxygen mixture (3.5% CH_4 and 7% O_2) in argon bath gas at 1600 K and 1 atm. Fig. 3(b) displays the absorption cross sections of these main combustion products as well as that of methane around 3403.4 nm at 296 K

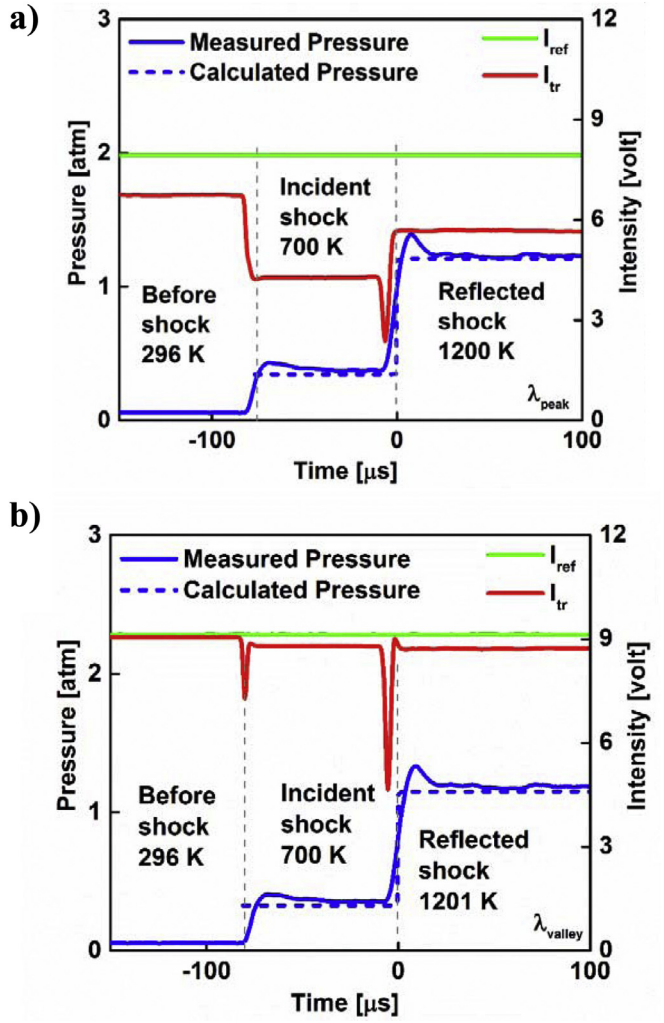

Fig. 4. Example reference and transmitted intensity traces as well as pressure measurements taken at the (a) peak and (b) valley wavelengths with an initial gas mixture of 2% CH_4 in Ar (Mixture 1).

and 1 atm. The cross section values were taken from the PNNL and HITRAN databases [23,24]. The main combustion products such as carbon-monoxide and carbon-dioxide have almost zero absorptivity, whereas the other species have relatively constant cross sections at the peak and valley wavelengths. Molecules such as H_2O, CO_2, C_2H_6, CH_2O, and C_2H_4 are species that can possibly interfere with the methane concentration measurements. In their shock tube study, Pyun et al. [10] reported the absorption cross sections of the aforementioned molecules at high temperatures around 1200 K and pressures between 0.7 and 1.6 atm (i.e. conditions were the same as the current study). They indicated that the aforementioned species have negligibly small differential absorptivity compared to that of methane. Water differential cross section, for example, is 0.002 m^2/mol at 1200 K, whereas methane differential cross section is 8 m^2/mol at the same conditions.

3.2. Methane absorption cross sections at high temperatures in argon bath gas

Fig. 4(a) shows traces of the reference and transmitted light intensities and pressure measured using a gas mixture of 2% CH_4 in argon (mixture 1) inside a shock tube. The laser was centered at the peak wavelength (3403.4 nm). The mixture was shock heated to 700 K behind the incident wave and then to 1200 K behind the reflected wave. The calculated pressure from the Rankine–Hugoniot relations [25] showed very good agreement with the measured pressure trace obtained using the pressure transducer. Fig. 4(b) displays the results at the valley wavelength (3403.7 nm).

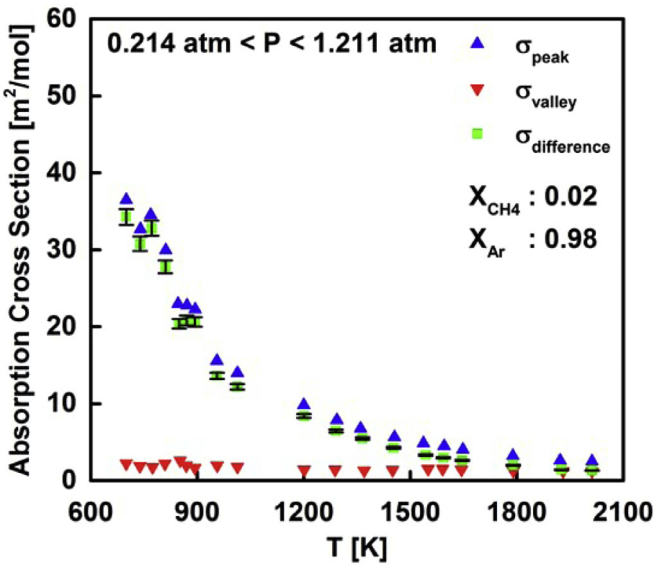

Fig. 5. Methane cross section vs. temperature. Mixture 1 (2% CH_4 in argon) was used for the measurements.

Absorption cross sections measured using 2% methane in argon at various temperatures and pressures are given in Fig. 5. The differential cross sections (peak-minus-valley) are also displayed. The following correlations were obtained using data taken behind the reflected shock waves

$$\sigma(T,P) = 5.41\left(\frac{1500}{T}\right)^{3.33}\left(\frac{1}{P}\right)^{0.76} \quad (2)$$

$$\sigma(T,P) = 3.86\left(\frac{1500}{T}\right)^{4.13}\left(\frac{1}{P}\right)^{0.76} \quad (3)$$

for the peak (Eq. (2)) and differential (Eq. (3)) cross sections, respectively.

3.3. Methane absorption cross sections at high temperatures in argon bath gas diluted with 30% carbon dioxide

Fig. 6(a) shows sample traces of the reference and transmitted light intensities and pressure measured using a gas mixture of 2% CH_4 and 30% CO_2 in argon. The laser was centered at the peak wavelength (3403.4 nm). The mixture was shock heated to T = 931 K behind the incident wave and then to 1614 K behind the reflected wave. The calculated pressure matched the measured one very well. Fig. 6(b) displays the results at the valley wavelength (3403.7 nm).

Absorption cross sections measured using 2% methane and 30% carbon dioxide in argon bath gas at various temperatures and pressures are given in Fig. 7. The following correlations were obtained using data taken behind the reflected shock waves

$$\sigma(T,P) = 5.14\left(\frac{1500}{T}\right)^{3.39}\left(\frac{1}{P}\right)^{0.76} \quad (4)$$

$$\sigma(T,P) = 3.57\left(\frac{1500}{T}\right)^{4.93}\left(\frac{1}{P}\right)^{0.76} \quad (5)$$

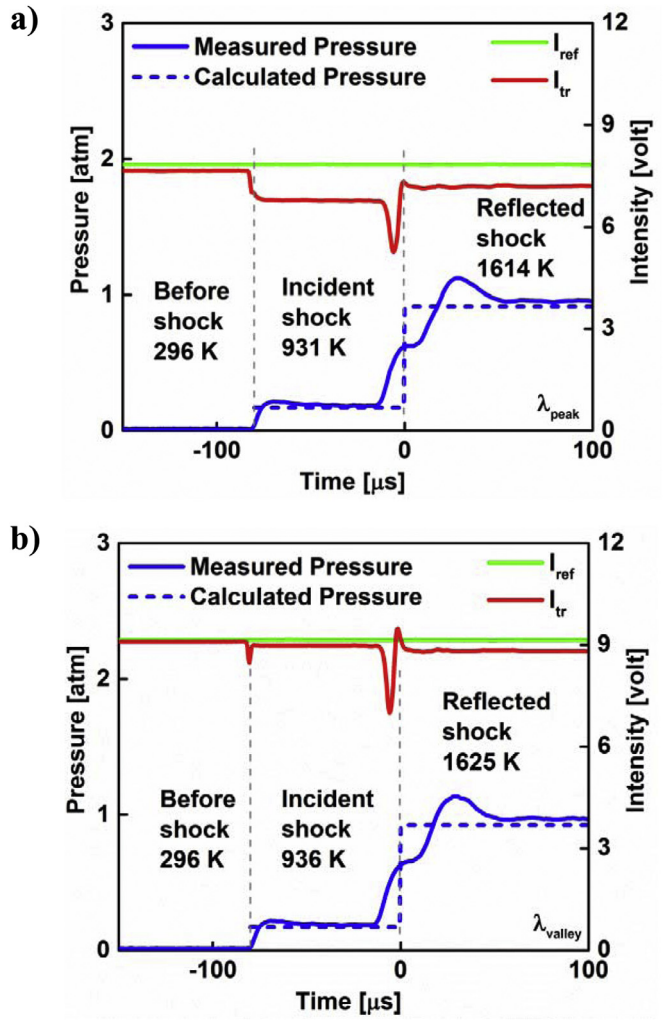

Fig. 6. (a) Example reference and transmitted intensity traces as well as pressure measurements taken at the (a) peak and (b) valley wavelengths with an initial gas mixture of 2% CH_4 and 30% CO_2 in Ar (Mixture 2).

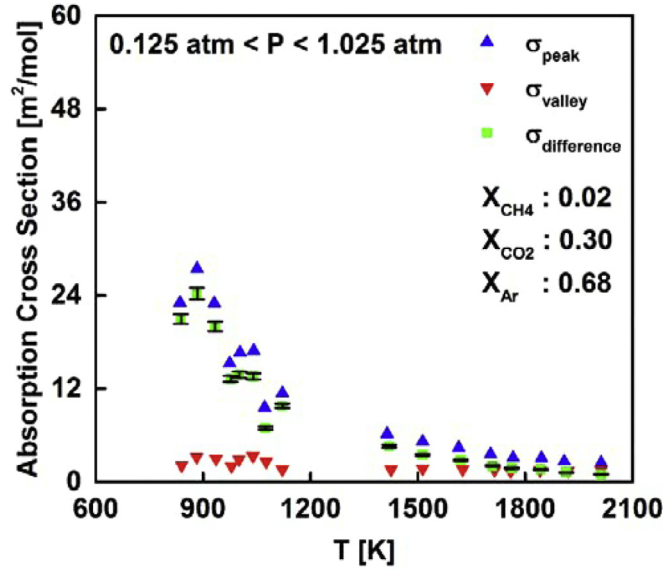

Fig. 7. Methane cross section vs. temperature. Mixture 2 (2% CH_4 and 30% CO_2 in argon) was used for the measurements.

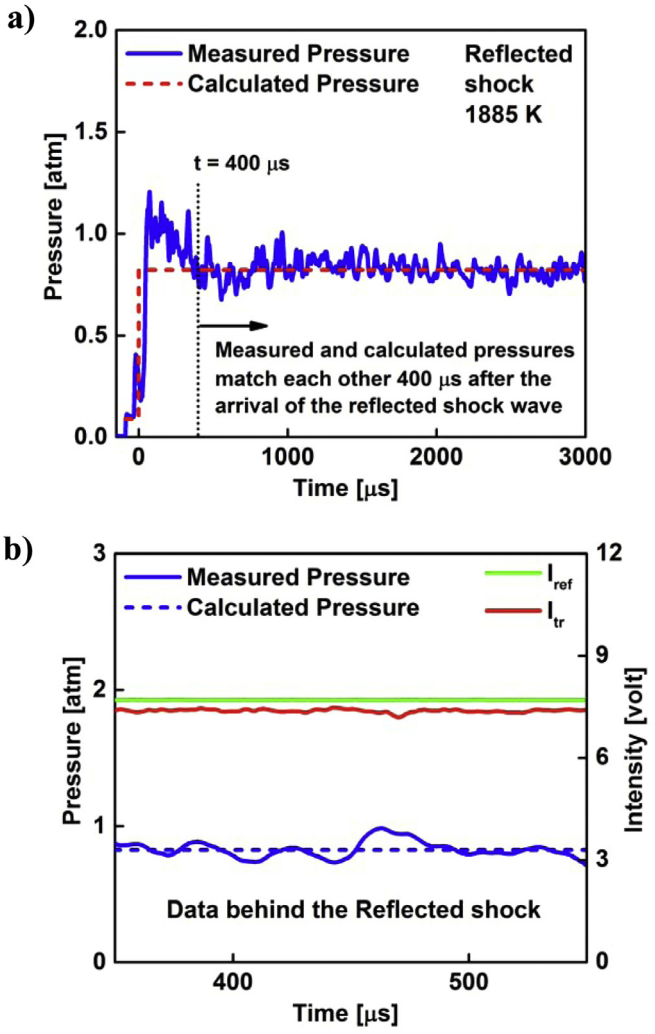

Fig. 8. (a) Comparison of measured and calculated pressures using 2% CH_4 and 98% CO_2 (Mixture 3), (b) the corresponding reference and transmitted intensity traces taken at the peak wavelength.

for the peak (Eq. (4)) and differential (Eq. (5)) cross sections, respectively.

3.4. Methane absorption cross sections at high temperatures in carbon dioxide bath gas

In Fig. 8(a) we compare the measured and calculated pressure profiles for one of the data points taken using 2% CH_4 and 98% CO_2. Severe bifurcation of the shock wave was observed for the experimental data taken using mixture 3. Bifurcation results in a big discrepancy between the measured and calculated pressure profiles at early time periods of the experiments. It happens when the boundary layer does not have sufficient momentum to pass through the normal reflected shock wave. The severity of it increases with the amount of di-atomic/polyatomic molecules in the test gas mixture [26,27]. Also, it depends on the γ (specific heat ratio) of the gas. The measured pressure profiles in Figs. 6 and 8(a) showed bifurcation due to the gas mixtures being comprised of 30 and 98% CO_2 gas ($\gamma_{CO2} = 1.28$), whereas no bifurcation was observed in Fig. 4 because of the use of monatomic Ar bath gas ($\gamma_{Ar} = 1.66$).

In their paper, Hanson and Petersen [27] discussed how to interpret the shock tube data when severe bifurcation of the shock wave happens. They indicated that the measured ignition delay

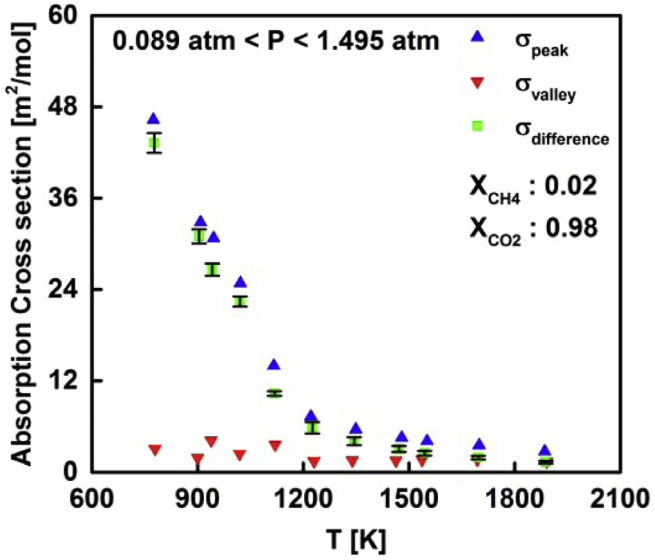

Fig. 9. Methane cross section vs. temperature. Mixture 3 (2% CH_4 in carbon-dioxide) was used for the measurements.

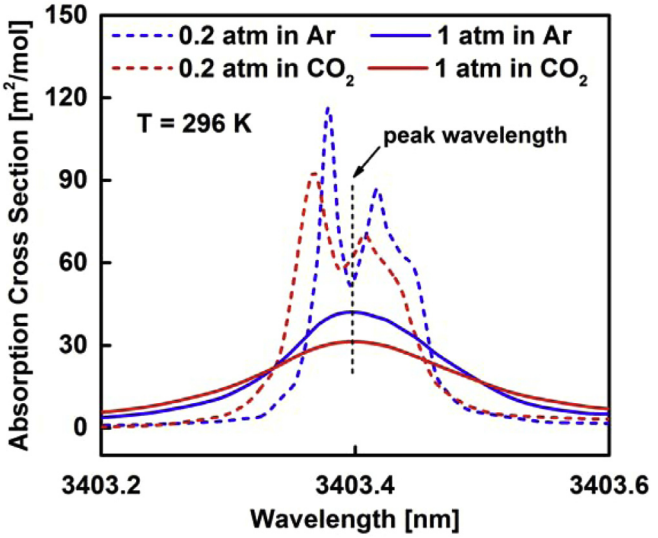

Fig. 10. Comparison of absorption cross sections of methane measured at low (0.2 atm) and high pressures (1 atm) using two different bath gasses: carbon dioxide and argon.

time data (or data of cross section, concentration, etc.) is not affected by the bifurcation, provided that the data points are taken in a temporal location where the measured and predicted pressure profiles match each other. In this study, a reasonable agreement between the two pressures was seen 400 μs after the arrival of the reflected shock wave. Therefore, we took the time average of the measured intensities (I_{ref} and I_{tr}) for 100 μs after this agreement was observed. The temporal onset of this agreement was nearly the same for different runs. Fig. 8(b) shows sample traces of the intensities and pressure obtained at the peak wavelength for an initial gas mixture of 2% CH_4 in carbon dioxide bath gas.

Absorption cross sections measured using 2% methane and 98% carbon dioxide at various temperatures and pressures are given in Fig. 9. The following correlations were obtained using data taken behind the reflected shock waves

$$\sigma(T,P) = 5.02\left(\frac{1500}{T}\right)^{3.16}\left(\frac{1}{P}\right)^{0.76} \tag{6}$$

$$\sigma(T,P) = 3.14\left(\frac{1500}{T}\right)^{4.44}\left(\frac{1}{P}\right)^{0.76} \tag{7}$$

for the peak (Eq. (6)) and differential (Eq. (7)) cross sections, respectively.

3.5. Discussion on the methane cross-sections at various CO_2 levels

The collisional width of an absorption transition, $\Delta\nu_C$, is given by

$$\Delta\nu_C = P\sum_A \chi_A 2\gamma_{B-A} \tag{8}$$

where $2\gamma_{B-A}$ is the broadening coefficient, B is the species of interest (i.e. CH_4), A is the perturber (i.e. CH_4, Ar, or CO_2) that broadens the absorption line of B, χ_A is the mole fraction, and P is the pressure. The absorption cross sections and the line shape profiles are dependent on each other according to Beer-Lambert law. The broadening coefficient and the absorption cross sections are inversely related to each other as discussed by Alrefae et al. [15]. They showed how methane absorption cross sections varied for measurement results taken using a HeNe laser at a fixed wavelength of 3.392 μm for three different bath gasses (He, Ar, and N_2). The mixture of CH_4/He had the highest cross section, followed by the other two: CH_4/Ar, and CH_4/N_2 mixtures. This was explained due to the differences in the broadening coefficients of CH_4 in He, Ar, and N_2, which were reported in earlier studies [28,29] as 0.048, 0.056, and 0.063 cm^{-1}/atm, respectively. The broadening coefficients of CH_4/Ar and CH_4/N_2 mixtures at 295 K and 3403.4 nm were reported by Pine [28] as 0.04576 and 0.05271 cm^{-1}/atm, respectively.

To the best of our knowledge there is no study in the literature on the broadening coefficients of CH_4/CO_2 mixtures at the wavelengths studied in the present work. Therefore, we performed absorption cross section measurements of methane in argon and carbon-dioxide gasses at low (0.2 atm) and high pressures (1 atm) and at room temperature (296 K) using our DFB-cascade laser. The results are shown in Fig. 10. The absorption cross sections measured in argon was higher than those in carbon dioxide at 1 atm, whereas the opposite trend was observed at 0.2 atm due to the deconvolution of the lines at lower pressures. Voight line shape profiles were fit to the measured spectra at 1 atm (not shown in the figures). We observed that the FWHM of the line centered at 3403.4 nm was 0.155 nm for measurements taken using Ar. However, it increased to 0.190 nm in the case of CO_2. The high temperature shock tube data exhibited similar behaviors at low and high pressures. This is discussed in Fig. 11.

Fig. 11 compares the high temperature absorption cross sections of methane at 3403.4 nm for three different gas mixtures: 2% CH_4 in bath gas of argon (mixture 1), 2% CH_4 in argon diluted with 30% carbon dioxide (mixture 2), and 2% CH_4 in 98% carbon dioxide (mixture 3). The data taken at low (0.09 atm < P < .34 atm) and high (0.75 atm < P < 1.2 atm) pressures are plotted on the left and right y-axis, respectively. At high pressures, cross sections decrease as the CO_2 amount is increased, whereas an opposite trend is seen for cross sections at low pressures. These results are all consistent with the trends observed in Fig. 10, where the data were taken at room temperature for two different pressures (0.2 atm and 1 atm). Note that the pressure behind the reflected shock wave is dependent on the thickness of the diaphragm as well as the molecular weight of the test gas used in the experiments. Although the former was fixed for all experiments, there were variations in the reflected shock pressures due to using different gas mixtures. Those variations in the reflected shock pressure could affect the results as

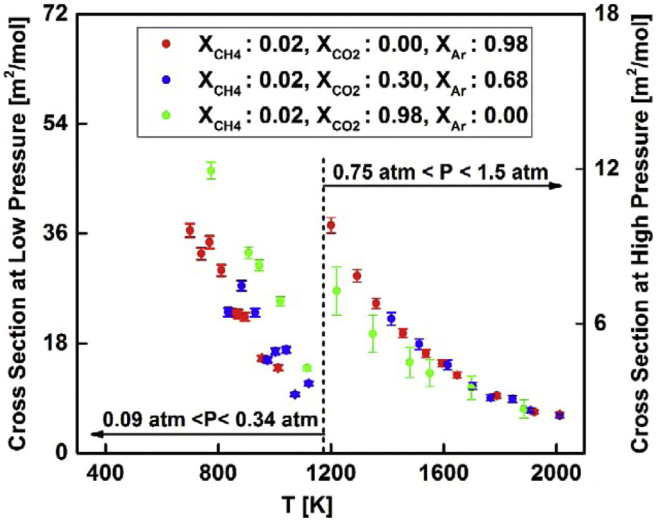

Fig. 11. Comparison of absorption cross section of methane at 3403.4 nm measured with 2% CH_4 in argon (Mixture 1), argon diluted with 30% CO_2 (Mixture 2), and in CO_2 (Mixture 3).

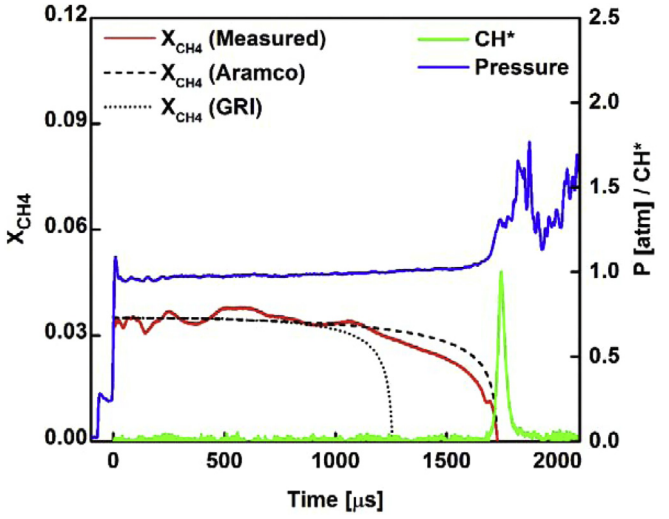

Fig. 12. Comparison of measured methane mole fraction time history with the predictions results obtained from GRI 3.0 and Aramco 1.3 mechanisms [21,32] (shown on the left y-axis) as well as the measured pressure and normalized CH* emission traces during the stoichiometric ignition of 3.5% CH_4 and 7% O_2 in argon bath at P ~ 1.0 atm and T = 1592 K (shown on the right y-axis).

well. For that reason, the exact values of cross sections and their corresponding experimental conditions are all given in Table A.1.

4. Applications of the measured cross section data

Empirical correlations of absorption cross sections Eqs. (3) and (5) can be utilized to determine concentrations of methane during oxy-methane combustion at high temperatures. Note that data taken behind the reflected shock waves were used to generate these correlations, because they are taken in the same temperature and pressure region of interest as in the combustion application. Also, the quality of the curve fits became much better when we excluded data taken behind the incident waves.

Recently, several research groups investigated the changes in the ignition characteristics of methane when CO_2 diluted gas mixtures were used during oxy-methane combustion [1,2,30,31]. The present authors [1] utilized laser absorption spectroscopy in a shock tube setup and determined methane concentrations during the ignition of methane in gas mixtures containing different percentages of CO_2 (0 and 30%). Those measurements were performed at the peak wavelength $\lambda_{peak} = 3403.4$ nm. It was seen that measured methane mole fraction (X_{CH4}) values did not decrease down to zero at the end of the ignition event. This was attributed to the absorption of light by some other hydrocarbons that were formed as methane depleted as a result of ignition. Accordingly, in the current study, we performed measurements at the peak and valley wavelengths and obtained an interference-free measurement by subtracting the absorbance measurement at the valley wavelength from the one taken at the peak wavelength. The results are discussed in the next two sections.

4.1. Methane concentration measurement in argon bath gas

Fig. 12 shows the pressure and CH_4 mole fraction time histories measured during the stoichiometric ignition of methane (3.5% CH_4 and 7% O_2 in Ar) at P ~ 1.0 atm and T = 1592 K. Also, the figure displays emission intensity results obtained from the CH* radical on the right hand side of the y-axis. The details of the emission measurements are given in previous publications [1]. Note that the cross section (and thus the mole fraction) was determined by subtracting the absorbance measurement taken at the valley wavelength from the one taken at the peak wavelength. Therefore, the temperature and pressure values used in determining the cross section were the average of the two measurements (e.g. $T_{peak} = 1591$ K and $T_{valley} = 1593$ K). The time of the steepest rise of the pressure and CH emission traces very well matched the time when methane mole fraction decreased to zero. In addition, comparisons of the experimental data with two different mechanism predictions are included in the figure. Simulations were run using the CHEMKIN PRO tool [22] based on the constant volume-internal energy (constant-U,V) assumption. GRI 3.0 and Aramco 1.3 mechanisms were used for the calculations [21,32].

The measured mole fraction time histories closely followed the Aramco 1.3 mechanism prediction results. Also, the figure clearly shows that methane mole fraction completely went down to zero. Therefore, the interferences were completely eliminated by means of the peak-minus-valley detection scheme. It was seen that the magnitude of the concentration fluctuations at the early stages of ignition was higher than 4500 ppm. This could be as a result of the increased noise due to the two-wavelength measurements performed using a single laser with multiple runs. For example, there were temperature variations between different runs. However, these variations were kept below 10 K, which were well within the uncertainty limits.

4.2. Methane concentration measurements in argon bath gas diluted with 30% carbon dioxide

Similar concentration measurements were performed for a stoichiometric mixture of 3.5% CH_4, 7% O_2, and 30% CO_2 in Ar at P ~ 1.0 atm and T = 1802 K. The results are shown in Fig. 13. Measured mole fraction time histories again closely followed the Aramco 1.3 mechanism prediction results. Similar to Fig. 12, the measured methane mole fraction completely went down to zero.

4.3. Uncertainties in the measurements of absorption cross-section and mole fraction

Based on the Beer lambert law (Eq. 1), the uncertainty in the cross-section measurement is dependent on the errors in the mea-

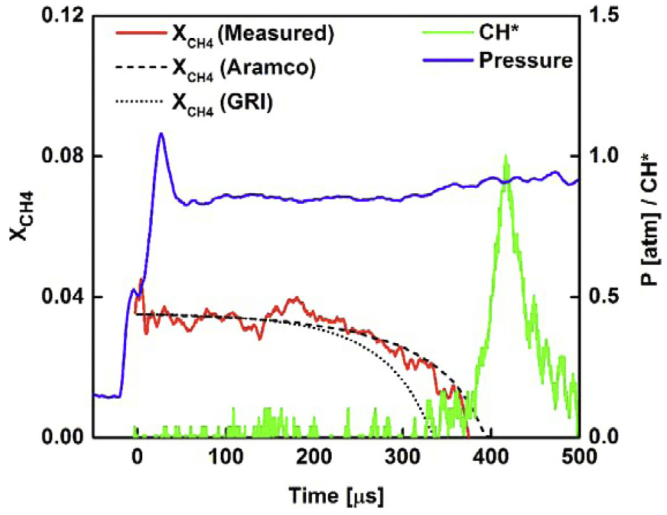

Fig. 13. Comparison of measured methane mole fraction time history with predictions results obtained from GRI 3.0 and Aramco 1.3 mechanisms [21,32] as well as the measured pressure and normalized CH* emission traces during the stoichiometric ignition of 3.5% CH_4, 7% O_2, 30% CO_2 in argon bath at P ~ 1.0 atm and T = 1802 K.

surements of absorbance, mole fraction, temperature, pressure, and path length. The temperature measurement accuracy (+/−2%) for shock tube data was extensively studied in the literature [33] and that is dependent on the measurement of the shock velocity. The uncertainty in the initial mole fraction (+/−0.2%) is dependent on the accuracies of the capacitance type manometers, which are +/−0.12%. The uncertainty in the path length was taken as +/−0.5 mm. The error in the measured absorbance is dependent on the mixture type and is taken as the standard deviation of the data as explained in the study of Alrefae et al. [15]. Although there was a good agreement between the measured and theoretically calculated pressures, the fluctuations observed for tests involving 98% CO_2 gas was rather big. Therefore, the error in the pressure measurement was also taken as the standard deviation of the data. The resulting uncertainties in the cross-section measurements were +/−3, +/−4, and and +/−13% for mixture 1 (Fig. 5), mixture 2 (Fig. 7), and mixture 3 (Fig. 9), respectively. The resulting uncertainties in the mole fraction measurements were+/−5 and+/−7% for data presented in Figs. 12 and 13, respectively. Note that the uncertainties of the cross-section data taken behind the incident shock wave were not dependent on the mixture type and they were+/−3%.

Methane mole fraction measurement results shown in Figs. 12 and 13 were obtained assuming constant temperature (T_5) and pressure (P_5) behind the reflected shock waves. However, the changes in T_5 and P_5 can influence the absorption cross-sections and thus the mole fraction of methane. Therefore, simulations were run using the CHEMKIN PRO tool [22] and the Aramco 1.3 Mechanism [21] based on the constant volume-internal energy (constant-U,V) assumption. A good agreement between the measured and predicted pressure profiles was seen. As a result, changes in the calculated mole fractions (using the cross-section data) due to variations in temperature and pressure behind the reflected shock waves were within the uncertainty limits.

5. Conclusions

The absorption cross sections of methane at two different wavelengths (λ_{peak} = 3403.4 nm and λ_{valley} = 3403.7 nm) were measured for three non-reactive gas mixtures: 2% CH_4 in Ar and 2% CH_4 in Ar diluted with 30% CO_2, and 2% CH_4 in CO_2. Present experiments were performed behind the incident and reflected shock waves at temperatures between 700 < T < 2000 K and pressures between 0.1 < P < 1.5 atm. The empirically obtained correlations indicated that the absorption cross sections of methane were lower when measured in CO_2 diluted gas mixtures at atmospheric pressures. Similar trends were observed according to the broadband room temperature (296 K) and atmospheric pressure measurements. However, an opposite trend was observed both at high and room temperatures when the measurements were taken at lower pressures (0.2 atm). This change was due to the deconvolution of the lines. Furthermore, two case studies were presented within this paper using the empirically obtained cross section correlations. They were applied for measuring methane concentration time histories during stoichiometric combustion of methane in argon bath gas with and without CO_2 dilution. The results were compared to the predictions of two kinetics models: GRI 3.0 and Aramco 1.3 mechanisms [21,32]. A very good agreement was seen with predictions obtained from the Aramco 1.3 mechanism.

Disclaimer

Acknowledgements

Donors of the American Chemical Society Petroleum Research Fund, Defense Threat Reduction Agency (Grant No. HDTRA1-16-1-0009), and Department of Energy (Grant No. DE-FE0025260) are acknowledged for partial financial support. B. Koroglu performed parts of this work under the auspices of the U.S. Department of Energy by Lawrence Livermore National Laboratory under Contract DEAC52-07NA27344.

Appendix

Table A.1.

Table A.1
Absorption cross sections of methane.

Mixture Type	T [K]	P [atm]	σ_{peak} [m^2/mol]	T [K]	P [atm]	σ_{valley} [m^2/mol]
Mixture I	1200	1.211	9.814	1201	1.148	1.421
	1293	1.213	7.864	1288	1.141	1.417
	1360	1.133	6.781	1370	1.145	1.313
	1455	1.064	5.636	1450	1.058	1.376
	1537	1.036	4.853	1550	1.048	1.521
	1595	0.903	4.472	1591	0.962	1.497
	1648	0.962	4.025	1644	0.959	1.408
	1789	0.926	3.221	1790	0.921	1.237
	1922	0.923	2.594	1930	0.928	1.200
	2012	0.887	2.492	2012	0.886	1.194
	700	0.344	36.487	700	0.327	2.236
	740	0.332	32.687	738	0.313	1.893
	769	0.303	34.554	774	0.305	1.743
	811	0.276	29.972	809	0.275	2.181
	846	0.262	22.974	852	0.265	2.594
	871	0.225	22.778	869	0.24	1.959
	894	0.237	22.276	893	0.236	1.642
	955	0.221	15.560	956	0.22	1.950
	1013	0.214	13.978	1013	0.214	1.787
Mixture II	1414	1.011	6.1922	1425	1.025	1.589
	1513	0.954	5.219	1513	0.958	1.727
	1614	0.915	4.414	1625	0.924	1.629
	1703	0.877	3.598	1714	0.887	1.529
	1766	0.862	3.136	1759	0.776	1.381
	1845	0.812	3.093	1841	0.84	1.477
	1909	0.781	2.646	1919	0.803	1.422
	2012	0.754	2.457	2012	0.74	1.474
	974	0.16	15.273	979	0.161	2.017
	931	0.17	23.025	936	0.172	2.986
	883	0.184	27.449	882	0.184	3.210
	835	0.201	23.092	840	0.203	2.132
	1003	0.154	16.654	1000	0.139	2.878
	1041	0.143	16.908	1039	0.148	3.329
	1121	0.128	11.416	1121	0.125	1.614
Mixture III	1221	1.47	7.275	1230	1.495	1.457
	1349	1.279	5.614	1339	1.258	1.546
	1479	1.22	4.519	1463	1.19	1.499
	1551	1.14	4.091	1537	1.131	1.625
	1699	1.037	3.533	1694	1.032	1.646
	1885	0.822	2.701	1891	0.828	1.378
	774	0.204	46.299	779	0.206	3.036
	908	0.15	32.821	900	0.148	1.840
	945	0.137	30.739	938	0.136	4.137
	1021	0.119	24.824	1019	0.118	2.416
	1116	0.089	13.942	1120	0.09	3.597

Supplementary materials

Supplementary material associated with this article can be found, in the online version, at doi:10.1016/j.jqsrt.2017.11.003.

References

[1] Koroglu B, Pryor OM, Lopez J, Nash L, Vasu SS. Shock tube ignition delay times and methane time-histories measurements during excess CO2 diluted oxy-methane combustion. Combust Flame 2016;164:152–63.

[2] Hargis JW, Petersen EL. Methane ignition in a shock tube with high levels of CO_2 dilution: consideration of the reflected-shock bifurcation. Energy Fuels 2015;29:7712–26.

[3] Pryor O, Barak S, Koroglu B, Ninnemann E, Vasu SS. Measurements and interpretation of shock tube ignition delay times in highly CO2 diluted mixtures using multiple diagnostics. Combust Flame 2017;180:63–76.

[4] Cai L, Kruse S, Felsmann D, Thies C, Yalamanchi KK, Pitsch H. Experimental design for discrimination of chemical kinetic models for oxy-methane combustion. Energy Fuels 2017;31:5533–42.

[5] Watanabe H, Shanbhogue SJ, Taamallah S, Chakroun NW, Ghoniem AF. The structure of swirl-stabilized turbulent premixed CH_4/air and $CH_4/O_2/CO_2$ flames and mechanisms of intense burning of oxy-flames. Combust Flame 2016;174:111–19.

[6] Sur R, Wang S, Sun K, Davidson DF, Jeffries JB, Hanson RK. High-sensitivity interference-free diagnostic for measurement of methane in shock tubes. J Quant Spectrosc Radiat Transf 2015;156:80–7.

[7] Sajid MB, Javed T, Farooq A. High-temperature measurements of methane and acetylene using quantum cascade laser absorption near 8 μm. J Quant Spectrosc Radiat Transf 2015;155:66–74.

[8] Lam K-Y, Ren W, Pyun SH, Farooq A, Davidson DF, Hanson RK. Multi-species time-history measurements during high-temperature acetone and 2-butanone pyrolysis. Proc Combust Inst 2013;34:607–15.

[9] Pyun SH, Ren W, Davidson DF, Hanson RK. Methane and ethylene time-history measurements in n-butane and n-heptane pyrolysis behind reflected shock waves. Fuel 2013;108:557–64.

[10] Pyun SH, Cho J, Davidson DF, Hanson RK. Interference-free mid-IR laser absorption detection of methane. Meas Sci Technol 2011;22.

[11] Koroglu B, Vasu SS. Measurements of propanal ignition delay times and species time histories using shock tube and laser absorption. Int J Chem Kinet 2016.

[12] Es-sebbar E-T, Farooq A. Intensities, broadening and narrowing parameters in the $\nu 3$ band of methane. J Quant Spectrosc Radiat Transf 2014;149:241–52.

[13] Lyulin OM, Petrova TM, Solodov AM, Solodov AA, Perevalov VI. Measurements of the broadening and shift parameters of methane spectral lines in the 5550–6140 cm−1 region induced by pressure of carbon dioxide. J Quant Spectrosc Radiat Transf 2014;147:164–70.

[14] Fissiaux L, Delière Q, Blanquet G, Robert S, Vandaele AC, Lepère M. CO_2-broadening coefficients in the $\nu 4$ fundamental band of methane at room temperature and application to CO_2-rich planetary atmospheres. J Mol Spectrosc 2014;297:35–40.

[15] Alrefae M, Es-sebbar E-T, Farooq A. Absorption cross-section measurements of methane, ethane, ethylene and methanol at high temperatures. J Mol Spectrosc 2014;303:8–14.

[16] Koroglu B, Loparo Z, Nath J, Peale RE, Vasu SS. Propionaldehyde infrared cross-sections and band strengths. J Quant Spectrosc Radiat Transfer 2015;152:107–13.

[17] Gaydon AG, Hurle IR. The shock tube in high-temperature chemical physics. NY: Reinhold Publishing Corp.; 1963.
[18] Koroglu B, Pryor O, Lopez J, Nash L, Vasu SS. Methane ignition delay times in CO_2 diluted mixtures in a shock tube. 51st AIAA/SAE/ASEE joint propulsion conference: American institute of aeronautics and astronautics; 2015.
[19] Pryor O, Barari G, Koroglu B, Lopez J, Nash L, Vasu SS. Shock tube ignition studies of advanced biofuels. 52nd AIAA/SAE/ASEE Joint propulsion conference: American institute of aeronautics and astronautics; 2016.
[20] Koroglu B, Pryor O, Lopez J, Nash L, Vasu SS. Shock tube ignition and CH_4 time-histories during propanal oxidation. 54th AIAA aerospace sciences meeting: American institute of aeronautics and astronautics; 2016.
[21] Metcalfe WK, Burke SM, Ahmed SS, Curran HJ. A hierarchical and comparative kinetic modeling study of $c1-c2$ hydrocarbon and oxygenated fuels. Int J Chem Kinet 2013;45:638–75.
[22] Chai M, Lu M, Liang F, Tzillah A, Dendramis N, Watson L. The use of biodiesel blends on a non-road generator and its impacts on ozone formation potentials based on carbonyl emissions. Environ Pollut 2013;178:159–65.
[23] Sharpe SW, Johnson TJ, Sams RL, Chu PM, Rhoderick GC, Johnson PA. Gas-phase databases for quantitative infrared spectroscopy. Appied Spectroscopy 2004;58:1452.
[24] Rothman LS, Gordon IE, Babikov Y, Barbe A, Chris Benner D, Bernath PF, et al. The HITRAN2012 molecular spectroscopic database. J Quant Spectrosc Radiat Transf 2013;130:4–50.
[25] Gaydon AG, Hurle IR. The shock tube in high-temperature chemical physics. New York: Reinhold; 1963.
[26] Strehlow RA, Cohen A. Limitations of the reflected shock technique for studying fast chemical reactions and its application to the observation of relaxation in nitrogen and oxygen. J Chem Phys 1959;30:257–65.
[27] Petersen EL, Hanson RK. Measurement of reflected-shock bifurcation over a wide range of gas composition and pressure. Shock Waves 2006;15:333–40.
[28] Pine AS. N_2 and Ar broadening and line mixing in the P and R branches of the v3 band of CH_4. J Quant Spectrosc Radiat Transf 1997;57:157–76.
[29] Mallard WG, Gardiner WC. Absorption of the 3.39 μm He-Ne laser line by methane from 300 to 2400 K. J Quant Spectrosc Radiat Transf 1978;20:135–49.
[30] Holton M, Gokulakrishnan P, Klassen M, Roby R, Jackson G. Autoignition delay time measurements of methane, ethane, and propane pure fuels and methane-based fuel blends. J Eng Gas Turbines Power 2010;132:091502.
[31] Almansour B, Thompson L, Lopez J, Barari G, Vasu SS. Laser ignition and flame speed measurements in oxy-methane mixtures diluted with CO2. J Energy Res Technol 2016;138:032201.
[32] Smith G.P., Golden D.M., Frenklach M., Moriarty N.W., Eiteneer B., Goldenberg M., et al. GRI-Mech 3.0. 1999.
[33] Herbon JT. Shock tube measurements of CH_3+O_2 kinetics and the heat of formation of the OH radical. Mechanical Engineering, Stanford University; 2004. Dissertation.